Fluoride-containing bioactive glasses: Effect of glass design and structure on degradation, pH and apatite formation in simulated body fluid

Brauer, DS; Karpulthina, N; O'Donnell, MD; Law, RV; Hill, RG

Fluoride-containing bioactive glasses: Effect of glass design and structure on degradation, pH and apatite formation in simulated body fluid

Delia S. Brauer[a,b,*], Natalia Karpukhina[c], Matthew D. O'Donnell[d], Robert V. Law[c], Robert G. Hill[b]

[a]Imperial College London, Department of Materials, Exhibition Road, London SW7 2AZ, UK

[b]Barts and The London, Unit of Dental Physical Sciences, Mile End Road, London E1 4NS, UK

[c]Imperial College London, Department of Chemistry, Exhibition Road, London SW7 2AZ, UK

[d]BioCeramic Therapeutics (BCT) Ltd., Incubator, Prince Consort Road, London SW7 2BP, UK

*Corresponding author. Tel.: +44 (0)207 882 7409; fax: +44 (0)207 882 7979. *E-mail address*: d.brauer@qmul.ac.uk.

Acta Biomaterialia 6 (2010) 3275–3282

Summary

Bioactive glasses are able to bond to bone through formation of carbonated hydroxyapatite in body fluids, and fluoride-releasing bioactive glasses are of interest for both orthopaedic and in particular dental applications for caries inhibition. Melt-derived glasses in the system SiO_2-P_2O_5-CaO-Na_2O with increasing amounts of CaF_2 were prepared by keeping network connectivity and the ratio of all other components constant.

pH change, ion release and apatite formation during immersion of glass powder in simulated body fluid at 37°C over up to two weeks were investigated. Crystal phases formed in SBF were characterised using infra-red spectroscopy, X-ray diffraction with Rietveld analysis and solid-state nuclear magnetic resonance spectroscopy (^{19}F and ^{31}P MAS-NMR). Results show that incorporation of fluoride resulted in a reduced pH rise in aqueous solutions compared to fluoride-free glasses and in formation of fluorapatite (FAp), which is more chemically stable than hydroxyapatite or carbonated hydroxyapatite and therefore is of interest for dental applications. However, for increasing fluoride content in the glass, fluorite (CaF_2) was formed at the expense of FAp. Apatite formation could be favoured by increasing the phosphate content in the glass, as the release of additional phosphate into the SBF would affect supersaturation in the solution and possibly favour formation of apatite.

Introduction

"Bioactive glass" is a generic term for a group of silicate glasses which have a highly disrupted structure (consisting of Q^2 silica chains with a large number of non-bridging oxygens – two per silicon tetrahedron), which degrade in aqueous solution and release ions such as calcium. These glasses are also known to form carbonated hydroxyapatite (HCA) *in vitro* in simulated body fluids (SBF), which have ionic concentrations close to human blood plasma [1], and this HCA layer is generally thought to facilitate attachment of proteins such as collagen, fibronectin and vitronectin which osteoblasts bind to and proliferate [2], thereby allowing for the formation of an intimate bond to bone [3].

Bioactive silicate glasses are of interest for use as bone grafts, implant coatings, in aluminium-free glass polyalkenoate (ionomer) bone cements [4] and even in dentifrices [5], and in all these applications addition of fluoride would be beneficial. Fluoride is well known to prevent dental cavities by inhibiting enamel and dentine demineralisation, enhancing remineralisation and inhibiting bacterial enzymes [6,7]. An important factor here is the formation of fluorapatite (FAp), which is more acid resistant than HCA, the main component of enamel and dentine.

The ability of bioactive glasses to form apatite in body fluids is also used in toothpaste for treating dentine hypersensitivity [5]. Dentine hypersensitivity is caused by dentinal tubules of root dentine being exposed. The toothpaste contains bioactive glass with a large fraction of particles small enough to enter the dentinal tubules. Formation of apatite then occludes the tubules and thus reduces sensitivity. Formation of FAp rather than HCA would be beneficial, as it is more chemically stable and would therefore less readily dissolve when the mouth is exposed to acidic conditions.

Fluoride is also known to increase bone density [8,9], and despite a narrow therapeutic window and some dispute on effectiveness in prevention of fractures [9,10] fluoride-releasing implants might be of interest for patients suffering from osteoporosis.

We recently characterised the structure of a series of glasses in the system SiO_2–P_2O_5–CaO–Na_2O with increasing concentrations of CaF_2 [11]. Network connectivity (NC) [12] was fixed at 2.13 by adding CaF_2 while the ratio of all other components was kept constant, assuming that fluoride stays associated with calcium, *i.e.* no Si-F bonds are formed [11,13]. Our hypothesis was that by keeping NC fixed we would not affect the degradability of the glasses and their ability to form apatite in SBF *in vitro*. We therefore performed degradation experiments in SBF and demonstrate the effects of glass composition and structure have on degradation, *in vitro* apatite formation and pH of fluoride-containing bioactive glasses. To our knowledge this is the first characterisation of apatite formed by bioactive glasses in simulated body fluid using ^{19}F and ^{31}P solid-state nuclear magnetic resonance.

Materials and methods

Glass synthesis

Glasses in the system SiO_2–P_2O_5–CaO–Na_2O were prepared using a melt–quench route. CaF_2 was added in increasing amounts while network connectivity (NC) and the ratio of all other components were kept constant (glasses A to G, Table 1). In addition, one sodium-free glass was synthesised (glass H, Table 1). Mixtures of analytical grade SiO_2 (Prince Minerals Ltd., UK), P_2O_5, $CaCO_3$, Na_2CO_3 and CaF_2 (all Sigma-Aldrich) were melted in a platinum-rhodium crucible for 1 h at 1430°C in an electric furnace (Lenton EHF 17/3). A batch size of approximately 100 g was used. After melting, the glasses were rapidly quenched into water to prevent crystallisation. After drying, the glass was ground using a vibratory mill (Glen Creston Gy-Ro mill) for 7 min and sieved to a particle size below 38 µm. All compositions were obtained in an amorphous state as confirmed by powder X-ray diffraction experiments (XRD; results not shown).

Table 1: Synthetic glass composition in mol% and theoretical network connectivity (NC).

Glass	SiO_2	P_2O_5	CaO	Na_2O	CaF_2	NC
A	49.47	1.07	23.08	26.38	-	2.13
B	47.12	1.02	21.98	25.13	4.75	2.13
C	44.88	0.97	20.94	23.93	9.28	2.13
D	42.73	0.92	19.94	22.79	13.62	2.13
E	40.68	0.88	18.98	21.69	17.76	2.13
F	36.83	0.80	17.18	19.64	25.54	2.13
G	33.29	0.72	15.53	17.75	32.71	2.13
H	44.88	0.97	44.87	-	9.28	2.13

pH and ion release in simulated body fluid (SBF)

Simulated body fluid was prepared using 7.996 g sodium chloride, 0.350 g $NaHCO_3$, 0.224 g potassium chloride, 0.228 g $K_2HPO_3 \times 3H_2O$, 0.305 g $MgCl_2 \times 6H_2O$, 0.368 g $CaCl_2 \times 2H_2O$, 0.071 g sodium sulfate, and 6.057 g tris(hydroxymethyl)amino methane, $(CH_2OH)_3CNH_2$, (Tris) per litre SBF, and pH was adjusted using 1 N hydrochloric acid (all chemicals Sigma-Aldrich) as described by Kokubo *et al*. [14]. SBF was kept at 37°C.

100 mL SBF were pipetted into 150 mL PE bottles. pH was measured using a pH meter (Oakton Instruments, NL) and 150 mg of glass powder (< 38 µm) were dispersed in the SBF, corresponding to a concentration of 1.5 g/L. Samples were placed in an orbital shaker at 37°C at an agitation rate of 60 rpm for 3 days, 1 week and 2 weeks. SBF from the same batch without glass powder was used as control. After removing the samples from the shaker pH was measured and solutions were filtered through medium porosity filter paper (5 µm particle retention, VWR International). Filter paper was dried at 37°C and the solutions were filtered sterile (0.2 µm cellulose acetate syringe filters, Anachem, UK) and kept at 4°C.

Undiluted solutions (for analysis of phosphorus) as well as samples diluted by a factor 1:200 (for sodium, results not shown) and 1:10 (for analysis of silicon, calcium, magnesium and potassium; results for magnesium and potassium not shown) were quantitatively analysed by inductively coupled plasma (ICP) emission spectroscopy (iCAP 6000, Thermo Scientific).

Fluoride-release into SBF was measured using a fluoride-selective electrode (Orion 9609BNWP with Orion pH/ISE meter 710, both Thermo Scientific). Calibration was performed using standard solutions prepared using SBF to account for ionic strength.

Characterisation of glass powders

Dried powders were analysed using Fourier-transform infrared spectroscopy (FTIR, Perkin-Elmer Spectrum GX, data collected from 1600 to 500 cm^{-1}) and XRD (Phillips PW1700, 40 kV/40 mA, CuKα, data collected at room temperature with a 0.04°2θ step and a count rate of 4 s per step, from 2θ values of 10° to 60°). For Rietveld analysis, Philips PC RD XRD files were converted to GSAS raw files using ConvX software. Rietveld analyses were performed using GSAS and EXPGUI software [15].

Structure was analysed using ^{19}F and ^{31}P magic angle spinning nuclear magnetic resonance (MAS-NMR). Experiments were performed using Bruker 200 MHz (4.7 T) and 600 MHz (14.1 T) spectrometers. ^{19}F NMR data were collected at a Larmor frequency of 188.2 MHz under spinning conditions of 12.5 kHz in a 4 mm rotor. To avoid ringing effects from the probe, the Hahn-echo pulse sequence $\pi/2-\tau-\pi$ was applied with a $\pi/2$ pulse of 2.35 μs and the echo delay τ of 40 μs. A recycle delay of 10 s was used, with 16 dummy scans performed before counting. A ^{19}F NMR background signal thoroughly acquired on the fluorine-free glass of this series was subtracted from the spectra of the fluorine-containing glasses. ^{19}F chemical shift scale was referenced using the -120 ppm peak of 1 M NaF aqueous solution as a secondary reference against $CFCl_3$. ^{31}P MAS-NMR spectra on glasses were acquired at 81.0 MHz in a 4 mm rotor spinning at 4.5 kHz. 64 transients of a single pulse experiment with 2.5 μs $\pi/2$ pulse and 49 s recycle delay were collected for each sample. ^{31}P MAS-NMR spectra on glass powders after soaking in SBF were collected at 242.9 MHz in a 4 mm rotor spinning at 6 to 7 kHz with a 30 s recycle delay and 8 scans before counting. ^{31}P chemical shift was referenced to 85% H_3PO_4. ^{19}F MAS-NMR spectra were fitted using dmfit software [16].

Results and Discussion

It is generally accepted that the formation of an apatite layer in body fluids facilitates attachment of osteoblasts (*via* proteins) on bioactive glasses (both *in vitro* and *in vivo*) and thereby enables bonding to bone [3]. While it is doubtful that the results of *in vitro* dipping tests in SBF can actually predict the behaviour of a material either during cell tests or

in vivo and has in fact produced false positive and false negative results [17], degradation experiments of bioactive glasses in SBF can give us insight into glass dissolution, pH changes and apatite formation in buffered solutions with ionic concentrations similar to those in human blood plasma. In addition, formation of apatite is of interest for dental applications.

We were particularly interested to see how glass composition, fluoride content and glass structure affect pH and apatite formation, as this information would enable us to design fluoride-containing bioactive glasses for specific applications. It is important to note that the glass system presented here is a model system which was not designed to give specific properties (*e.g*. high bioactivity) but was solely designed to help us understand the structure/property relationship in this type of biomaterial.

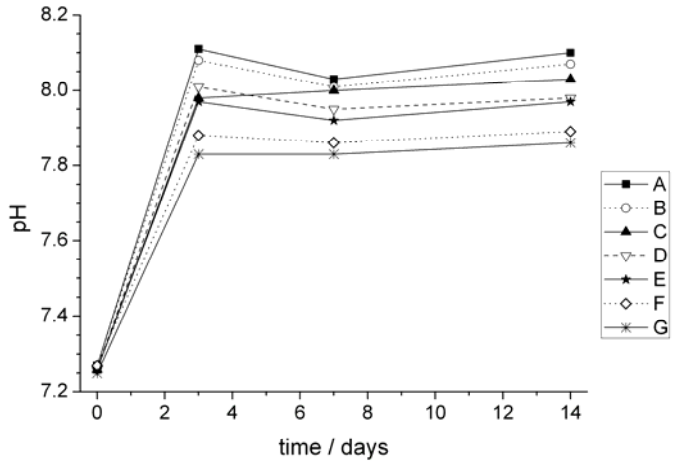

Figure 1. pH in SBF over two weeks of immersion of glass powder for glasses with increasing fluoride content (A to G). (Error is ± 0.03. Lines are drawn as a guide to the eye.)

Effect of fluoride content on pH of SBF

Soda-lime phosphosilicate-based bioactive glasses are well known to cause a pH rise upon immersion in aqueous solutions which favours apatite deposition in SBF but can negatively affect the surrounding tissue *in vivo*. The fluoride-releasing glasses in this work clearly showed a pH rise during the first three days of immersion in SBF from about 7.27 (the initial pH of the SBF) to up to over 8 (Fig. 1). After this initial pH increase the pH stayed constant over the remaining two weeks of the experiment. The pH rise, however, was less pronounced for increasing fluoride content in the glass (Fig. 2), as fluoride-free glass A gave a pH of 8.03 at one week while glass G, which has the highest CaF_2 content (33 mol%), gave a pH of 7.83. Sodium-free glass H gave a pH of 7.95 at one week (not shown).

The effect of the fluoride content of the glass on the pH in aqueous solution can be explained by ion exchange processes on the glass surface. Cations such as Na^+ or Ca^{2+} near the glass surface can go into solution in exchange for H^+ ions from the solution (from dissociation of water into H^+ and OH^-), which results in a pH increase. Similarly, F^- ions can be exchanged for OH^- ions, removing hydroxyl ions from solution and providing fluoride ions which buffer the effect of alkali ion release; so that for increasing fluoride content in the glass the pH rise is less pronounced.

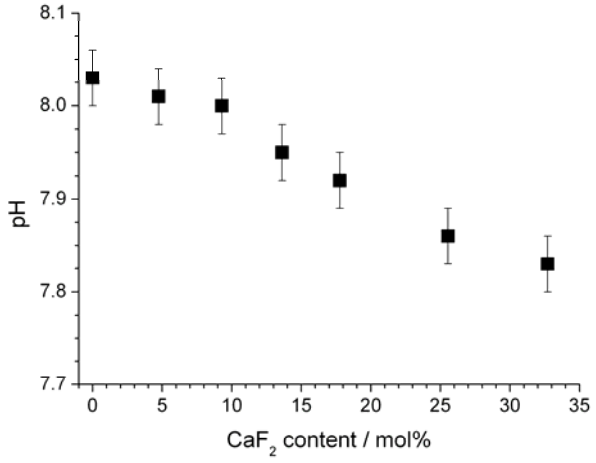

Figure 2. pH of SBF *vs*. CaF_2 content in the glass at 1 week immersion of glass powder for glasses with increasing fluoride content (A to G).

Apatite deposition in SBF

As the formation of apatite in SBF is strongly pH dependent [18], and the pH rise in SBF is less pronounced with increasing fluoride content in the glass, it might therefore be expected that the deposition of apatite in SBF decreases with increasing fluoride content in the glass. However, fluoride might be incorporated into the apatite to form fluorapatite, and as fluoroapatite has a much lower solubility than HCA and is stable at a lower pH, this might counterbalance the pH changes. We therefore followed the formation of apatite using FTIR, XRD and solid-state NMR.

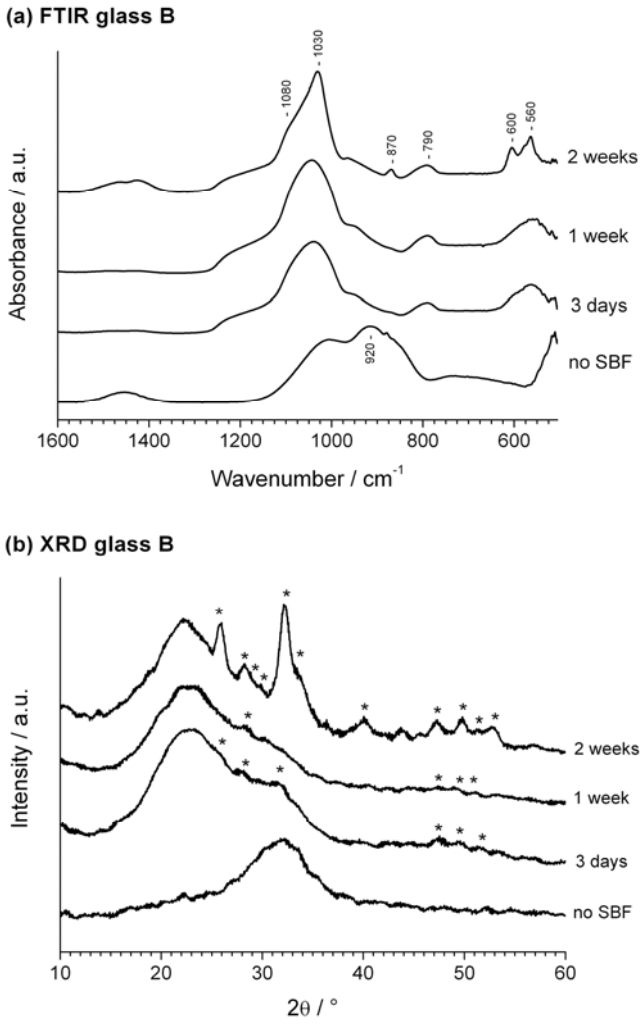

Figure 3. (a) FTIR spectra and (b) XRD patterns of untreated glass B (bottom) and after immersion in SBF for 3 days, 1 week and 2 weeks. Crystal phase in XRD pattern is apatite (∗).

FTIR spectra of all glass compositions showed significant changes after immersion in SBF for 3 days and longer in comparison to the spectrum of the unreacted glass (shown in Fig. 3a for glass B). The bands for the untreated glass powder were mostly due to Si-O vibrational modes: Si-O stretch, Si-O alkali stretch and Si-O bend [19]: After immersion in SBF all spectra showed the following changes (Figs. 3a and 4a): disappearance of the NBO (non-bridging oxygens, $Si\text{-}O^{-}$ $alkali^{+}$) band at 920 cm^{-1} and sharpening of the Si-O-Si stretch band at about 1030 cm^{-1}. At the same time, new bands appeared at about 790 cm^{-1}, which we assigned to Si-O-Si bond vibration between two adjacent SiO_4 tetrahedra. These changes indicate formation of a silica-gel surface layer after leaching of Ca^{2+} and Na^{+} ions and formation of Si-OH. Spectra after SBF immersion showed either a single peak or a split peak at approximately 560 cm^{-1}. This is the most characteristic region for apatite and other phosphates, and it corresponds to P-O bonding vibrations in a PO_4^{3-} tetrahedron and indicates presence of crystalline calcium phosphates including HAp and HCA [19]. A single peak in this region suggests presence of non-apatitic or amorphous calcium phosphate (ACP) which is

usually taken as indication of presence of precursors to hydroxyapatite (HAp) [20]. Apatitic PO_4^{3-} groups give characteristic split bands at 560 and 600 cm^{-1} [21], with a third signal at 575 cm^{-1} [22] observed for crystallites of small size. At one week (Fig. 4a), this split phosphate peak is most clearly pronounced for fluoride-free glass A, it is not present for glass B, and from glass C to G it gets more pronounced with increasing fluoride content. This suggests that small additions of fluoride affect apatite formation in SBF.

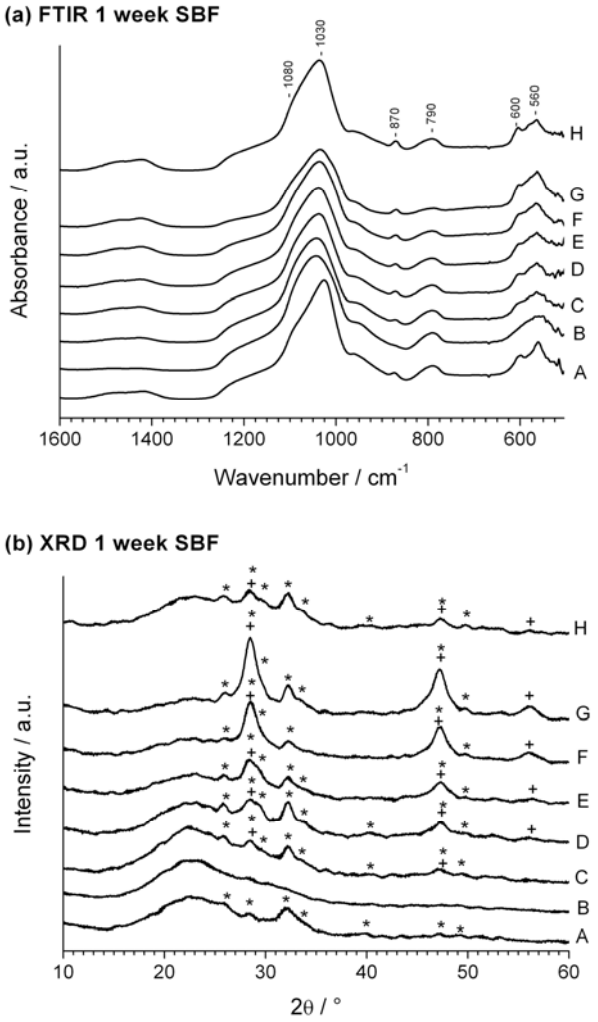

Figure 4. (a) FTIR spectra and (b) XRD patterns of glasses with increasing fluoride content (glasses A to G) and sodium-free glass H at 1 week immersion in SBF. Crystal phase in XRD pattern are calcium fluoride (+) and apatite (∗).

Presence of carbonate substitution in the apatite is indicated by the peak at about 870 cm^{-1} present in glasses A and C to H after 1 week immersion in SBF (Fig. 4a) and in glass B after 2 weeks in SBF (Fig. 3a). In SBF treated glass, this carbonate peak is usually taken as an indication for carbonate being incorporated into the apatite, resulting in HCA rather than stoichiometric HAp [18]. It is difficult to distinguish whether this band is split, in which case it would be B-type substitution (*i.e.* replacing a phosphate group). However, for most of the compositions treated in SBF for 1 week

(Fig. 4a) and 2 weeks (3a) broad CO_3^{2-} bands are present in the region starting from 1410 cm^{-1} which indicates B-type substitution. The CO_3^{2-} signal for A-type substitution would be shifted to higher wavenumbers, starting from 1460 cm^{-1}. The carbonates peaks are absent in glass B after 1 week in SBF (Figs. 3a and 4a) which is consistent with the absence of apatitic PO_4^{3-} bands [18,21].

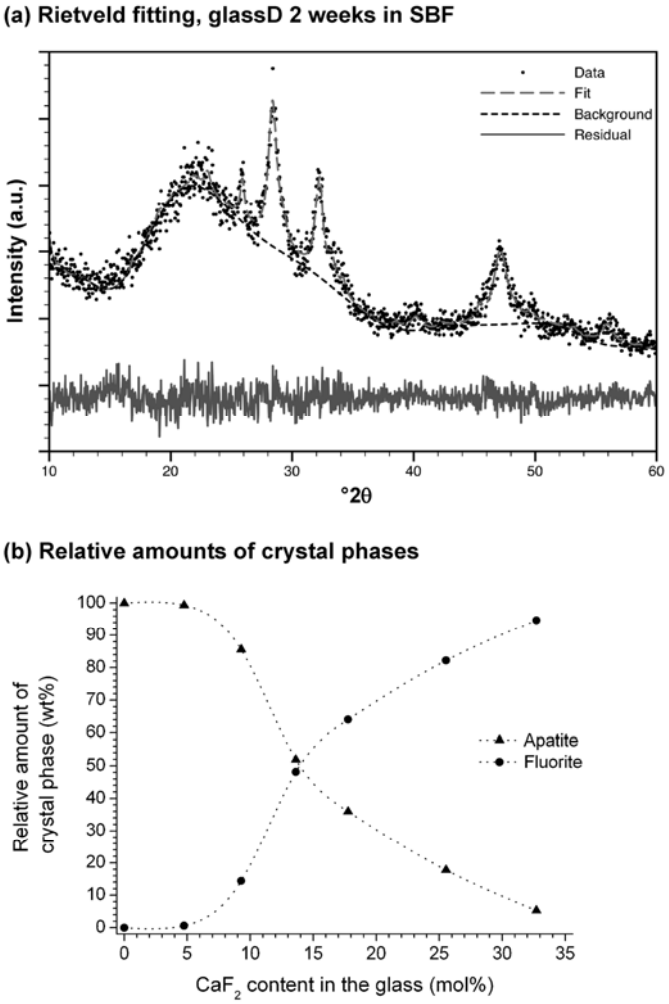

Figure 5. (a) Rietveld fitting of glass D at two weeks in SBF and (b) relative amount of crystal phases at 2 weeks in SBF according to Rietveld analysis *vs*. CaF_2 content in the glass at 2 weeks immersion in SBF for glasses with increasing fluoride content (A to G). (Lines are drawn as a guide to the eye.)

Spectra also showed a shoulder at 1080 to 1090 cm^{-1} which corresponds to a P-O stretch which is also observed in B-type substituted HCA [21]. At 1 week, it is most clearly pronounced in glasses A and high fluorine-content glasses (Fig. 4a), while in glass B it becomes more pronounced at 2 weeks (Fig. 3a).

Fig. 3b shows XRD patterns of glass B before SBF treatment and at three days, one week and two weeks of SBF immersion. All experimental XRD patterns were compared to reference patterns of hydroxyapatite (JCPDS 09-432),

fluorapatite (15-876), carbonated hydroxyapatite (JCPD 19-272) and carbonated fluorapatite (JCPDS 31-267); however, as these patterns overlap we will refer to the pattern of hydroxyapatite in the following. At three days small peaks at 26, 28, 32, 33, 47, 50 and 52 °2θ (JCPDS 9-432) indicate presence of apatite; these peaks are superimposed on an amorphous halo. The position of this amorphous halo has shifted compared to the unreacted glass, due to formation of an ion-depleted glass. The apatite peaks at one week are less pronounced than at three days due to a lower initial pH of the SBF (7.24 instead of 7.27), which suggests that formation of apatite for this glass composition is very susceptible to slight pH changes. At two weeks, peaks become clearly pronounced and additional reflections become visible; however, the lines remain very broad which indicates small size and highly disordered character of the crystals. This is typical for apatites precipitated from glass soaked in SBF [23]. Clear appearance of apatite Bragg's reflections after 2 weeks is consistent with presence of characteristic apatitic features on FTIR spectra of this glass (Fig. 3a).

Fig. 4b shows that at one week all glasses (except B) clearly show presence of apatite by XRD. However, for increasing fluoride content peaks of fluorite (CaF_2) at 28, 47 and 56 °2θ dominate the XRD pattern. Spectra were fitted using Rietveld analysis (Fig. 5a); plotting the results for relative amounts of crystal phases (Fig. 5b) shows sigmoidal curves of increasing relative amounts of fluorite with increasing CaF_2 content in the glass, while the relative amount of apatite decreases. This can be explained by the fact that the glasses in this series have low phosphate contents (1.07 mol% or less) which favours formation of CaF_2 rather than apatite, as we have an excess of calcium and fluoride ions, but not enough phosphate [23]. Crystallite size analysis using the Scherrer equation gave crystallite sizes between 4 and 20 nm. However, this only considers line broadening due to particle size reduction, while partial substitutions and resulting variations in lattice parameters will also broaden the lines and thereby affect crystallite size calculations. Crystallite size analysis of apatite formed on bioactive glasses in SBF previously showed crystal sizes in the range of 16 to 26 nm [23], and crystallites in our study are also likely to be in the nanometer size range (below 50 nm).

SBF-treated glass powders were analysed using ^{31}P and ^{19}F MAS-NMR, and Fig. 6 shows ^{31}P MAS-NMR results for untreated glass powder and for glass powder after immersion in SBF. Both before and after SBF treatment phosphate is present as orthophosphate. In the untreated glass the chemical shift of the orthophosphate peak moved from 9 ppm (glass A) to 3 ppm (glass H) with increasing CaF_2 content in the glass (Fig. 6c) which we explained by changes in the Ca/Na ratio charge balancing orthophosphate [11]. After SBF treatment of two weeks, however, we see broad signals with a chemical shift of around 3 ppm for all glass compositions (Fig. 6a). The average width of the line at 3 ppm, 730 Hz, is much broader than in crystalline apatite, about 120 Hz. This broadening of the ^{31}P MAS NMR signal for precipitated nanocrystalline apatite was studied by Jäger *et al*. [24]. This study reveals that the broadening is due to a disordered phase of calcium phosphates that covers the core of apatite nanocrystals. This disordered phase is often regarded as an apatite precursor. However, in our case for glasses after SBF treatment carbonate substitution is clearly

detected from FTIR, and this carbonate substitution together with probable fluorine incorporation are additional line broadening factors for ^{31}P MAS NMR spectra.

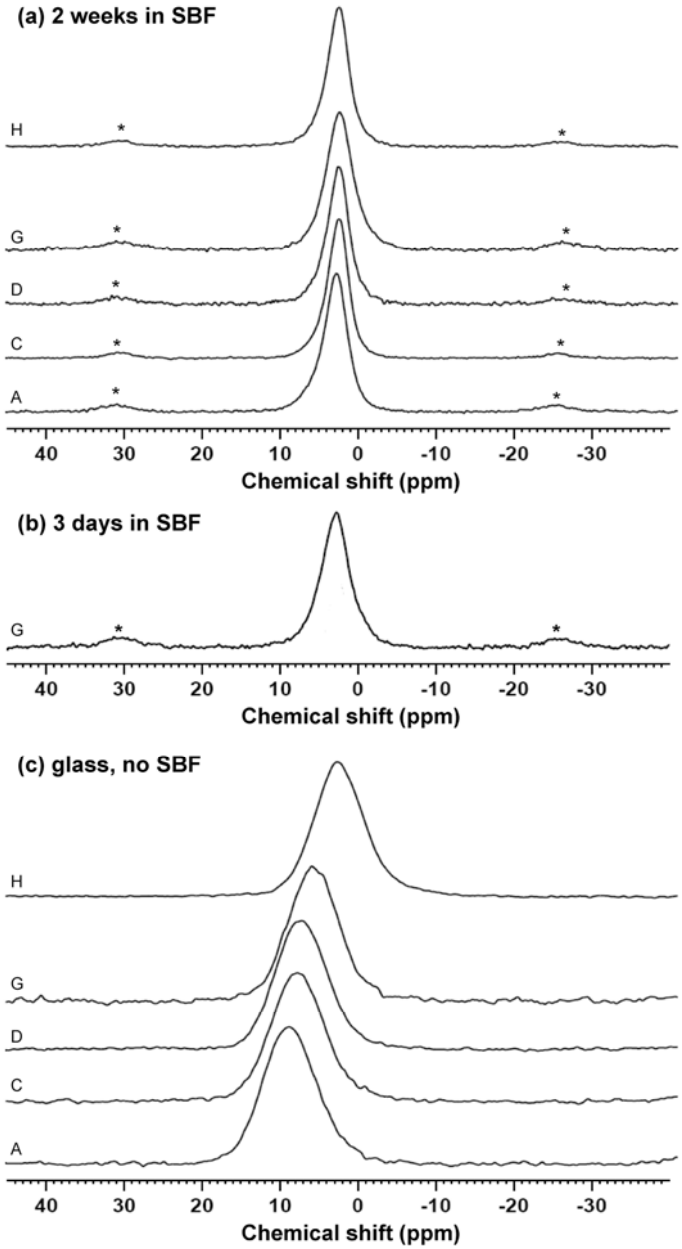

Figure 6. ^{31}P MAS-NMR spectra of glasses (a) after 2 weeks in SBF, (b) after 3 days (shown for glass G only) and (c) before SBF treatment. Spinning side bands are marked by an asterisk.

Additionally, the ^{31}P NMR peaks in Fig. 6a are asymmetric, which is particularly pronounced for F-free glass A. We estimated by deconvolution [16] that this asymmetry is due to a broad signal at 5-6 ppm for compositions A, C, D and H, with glass A showing the highest relative amount (~15%) of this additional phase. This additional feature is different from the initial glass signal and is also observed for sodium-free glass H. We assume that it could arise from mixed calcium sodium phosphates, presumably amorphous, absorbed on the glass surface while soaking in SBF. The

asymmetry largely disappears in the highest F containing glass G and the signal is broader compared to the other compositions in Fig. 6a after 2 weeks in SBF. The width of the ^{31}P NMR line for glass G after 3 days in SBF (Fig. 6b) was even broader than for the same glass after 2 weeks due to presence of the residual glass signal at around 6ppm. This implies that phosphates both from the glass and from SBF take part in the process of apatite formation in these glasses.

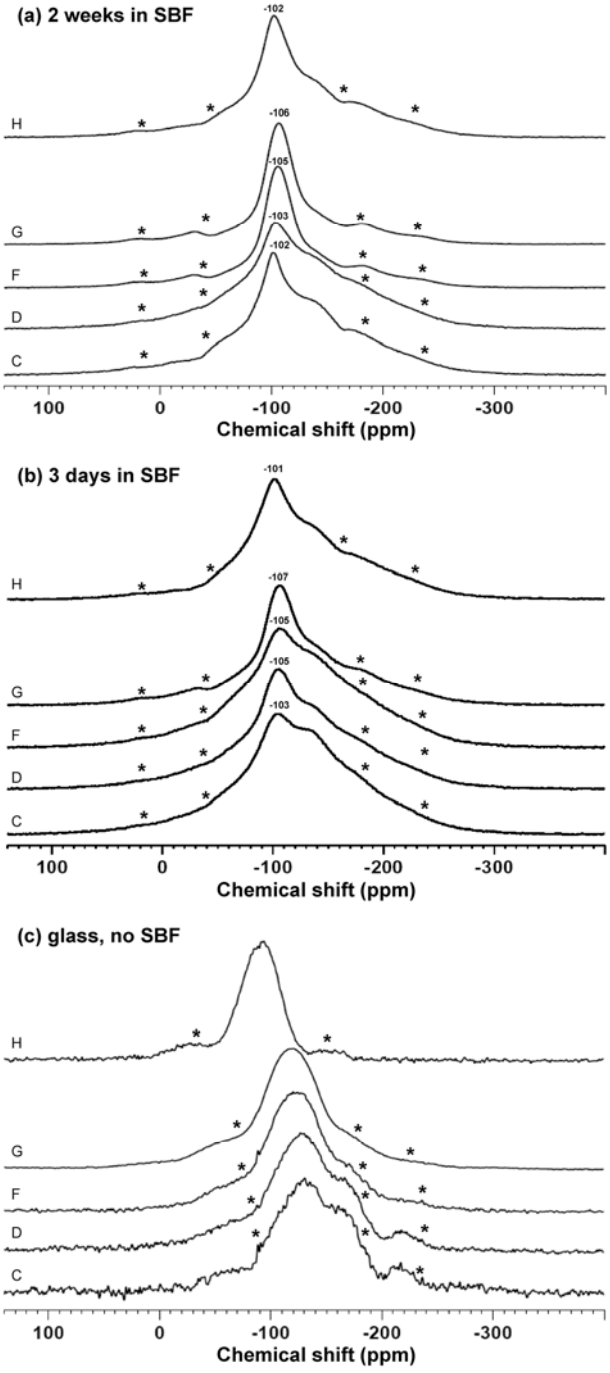

Figure 7. ^{19}F MAS-NMR spectra of glasses (a) after 2 weeks in SBF, (b) after 3 days in SBF and (c) without SBF treatment. Approximate position of spinning side bands of 12.5 kHz spinning speed are marked by an asterisk.

To clarify whether fluoride contents in the glass result in formation of FAp in addition to/rather than HCA (as the XRD pattern overlap and we therefore cannot distinguish between these two phases by using XRD alone), ^{19}F MAS NMR was run on SBF-treated glasses. Fig. 7 shows ^{19}F MAS-NMR spectra for both untreated glass and glass powder after immersion in SBF for 2 weeks (Fig. 7a) and 3 days (Fig. 7b). Apart from the sodium-free glass (H) all compositions showed presence of mixed sodium calcium fluoride species in the untreated glass [11]. The sodium-free glass (H) gives a single peak at -89 ppm corresponding to F-Ca(n) species (Fig. 7b).

After SBF treatment all glasses show a new feature between -101 ppm and -107 ppm and a broad shoulder on the low frequency side (right hand side) of the spectra. The main feature becomes more prominent after 2 weeks, and the broad low frequency shoulder decreases in intensity. This signal between -101 ppm to -107 ppm we assigned as an overlap between fluorapatite (-103 ppm) and fluorite (-108 ppm). The fraction of the latter increases in the glasses with high CaF_2 content, leading to a more negative overall shift. This is in agreement with the results of Rietveld analysis. The broad signal at about -140 ppm to -150 ppm can arise from mixed Ca/Na fluorine complexes adsorbed on the glass powder. This could be due to interaction of cations from the SBF solution, in particular sodium, with fluoride ions released from the glass during its dissolution. The proportion of this species decreases with time due to consumption of fluorine for formation of fluorapatite and fluorite. Additionally, the low frequency broad feature, for instance in glass C, could be partially caused by the residual glass phase. As an alternative explanation for the signal in this region we do not exclude presence of Si-F linkages resulting from adsorption of fluoride ions to the silca-gel surface layer.

Glass dissolution and ion release in SBF

Experimental concentration of phosphorus in SBF was (21.6 ± 0.1) mg/L (theoretical: 30.9 mg/L) and of calcium was (84.1 ± 1.4) mg/L (theoretical: 100.3 mg/L). These differences might be caused by precipitation of apatite in SBF without added glass powder, although no precipitate was visible. Alternatively, hydration of chemicals during storage used for preparation of SBF could have resulted in lower actual concentrations in the solution.

Fig. 8 shows ionic concentrations in SBF after immersion of glass powder for 1 week. For all glass composition, the phosphate concentration drops sharply compared to SBF (Fig. 8a). This is caused by formation of apatite (the Ca-P phase has started to form by 3 days according to XRD and FTIR): The glasses in this series have low phosphate contents, so phosphate ions from the SBF are used during formation of apatite. The considerable differences in phosphate concentrations between glass compositions can be explained by differences in formation of apatite. Glasses which formed apatite most readily (A, F to H) give the lowest phosphate concentration in SBF. Glass B, on the other hand, which showed no split FTIR phosphate peak and had the lowest XRD peak intensity at one week in SBF, gives the highest phosphate concentration in SBF.

At one week, Si has reached the solubility limit (around 60 mg/L with SiO_2 having a solubility of 0.12g/L in water) for all glasses (Fig. 8b). When silicon reaches the solubility limit, the phosphate concentration drops, and apatite is formed as formation of a silica gel layer is thought to aid nucleation of apatite. Calcium concentration in SBF decreases with increasing CaF_2 content from glass B to G (Fig. 8c), which can be explained by calcium ions being used up during formation of apatite and fluorite. Sodium-free glass H gives the highest calcium concentration in SBF, which is due to a higher calcium content in the glass.

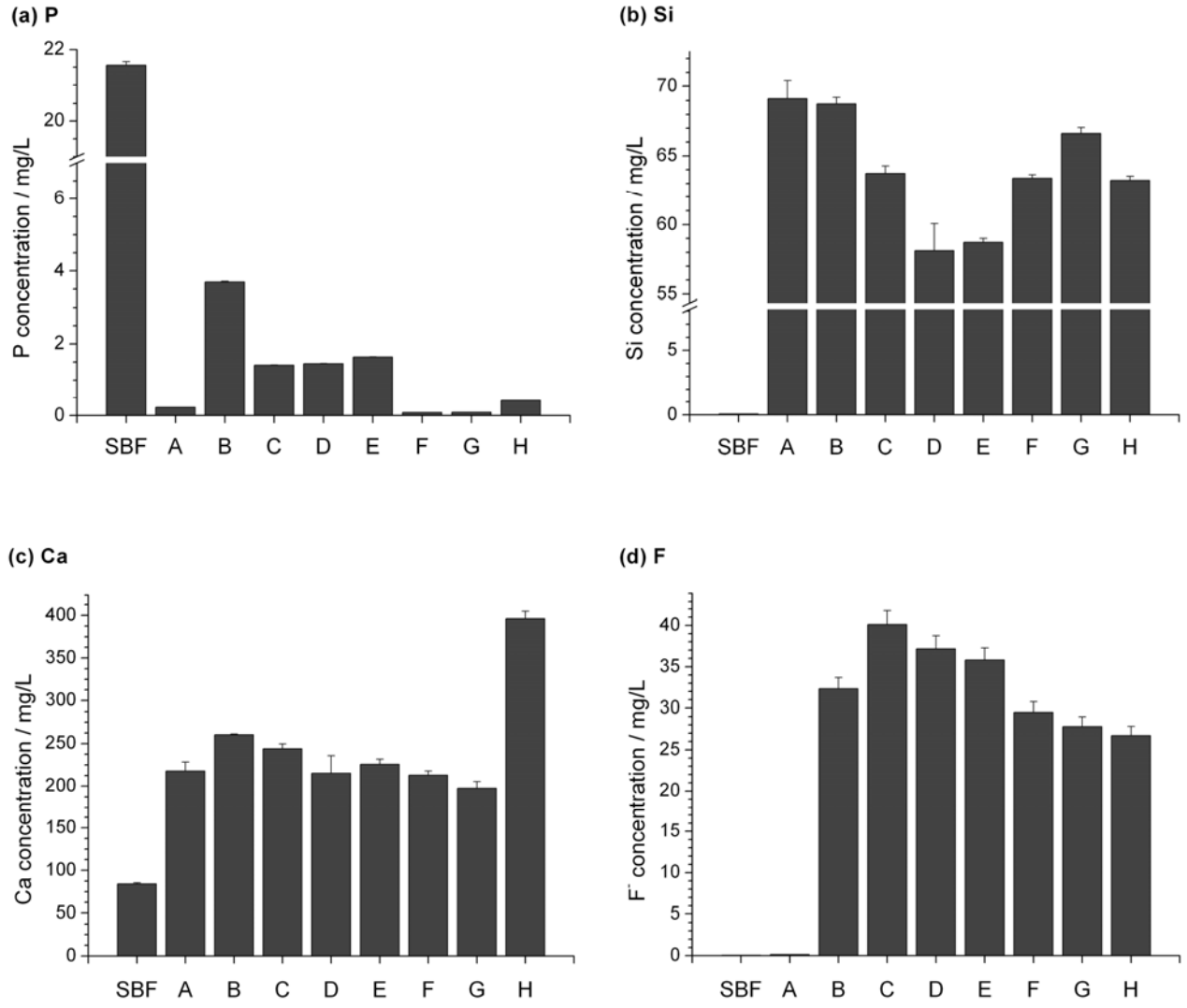

Figure 8. Concentrations of (a) phosphorus, (b) silicon, (c) calcium and (d) fluoride in SBF at 1 week immersion of glass powder for glasses with increasing fluoride content (A to G), a sodium-free glass (H) and SBF without addition of glass powder as control.

Fig. 8d shows that fluoride release does not increase with increasing fluoride content in the glass: Fluoride concentration in SBF was higher for glass C than for B (due to a higher CaF_2 content in the glass) but decreased from

glass C to H. Again, this can be explained by formation of FAp and fluorite. As both FAp and fluorite have a very low solubility in water, fluoride release decreases despite a higher fluoride concentration in the glass.

For dental applications, it is often implied that an increase in fluoride release from dental materials is better for caries prevention and formation of fluorapatite. However, our results show that high fluoride release might result in formation of fluorite rather than fluorapatite, but can also have negative effects such as a local drop in pH. Rather than increasing the fluoride-content in a ceramic material, it is important to a) design a composition which forms FAp rather than fluorite while releasing fluoride and b) to analyse the products formed in SBF in detail.

Fluoride-containing bioactive glasses in the literature

Bioactive glasses and ceramics are used as biomaterials for the repair of bone tissue, and fluoride-releasing bioactive glasses are of interest in both orthopaedic and dental applications due to their ability to form fluorapatite in body fluids. A number of publications investigate the ability of fluoride-containing bioactive glasses to form apatite in SBF [19,25-27]. Fujii *et al*. [25] tested fluoride-containing bioactive glasses in SBF and performed XRD on the SBF-treated samples. They assigned the XRD peak at 28°2θ HAp; however, the XRD patterns show that its intensity is enhanced. The main peaks to be expected for fluorapatite (JCPDS 15-876) are 31.9 (100% relative intensity), 33.1 (60%), 32.3 (55%) and 25.9 (40%). The peaks at 28.2 and 29.1°2θ only have relative intensities of 14 and 18%, respectively. Unless the structure shows orientation, we expect the experimental intensities in XRD to match the theoretical ones. The large peak at 28°2θ might therefore be caused by overlapping peaks of apatite and fluorite, which suggests that fluorite is formed as well as apatite. Similar trends can be seen by fluoride-containing 45S5-based bioactive glasses by Hench *et al*. [26]. This suggests that fluoride-release from bioactive glasses often results in formation of fluorite in addition to FAp or HAp but presence of fluorite will remain undetected if SBF-treated samples are only analysed using FTIR (as is done in many publications, e.g. by Kim *et al*. [19]), or if XRD patterns are only recorded for 2θ values of 40° or less (thereby missing the fluorite peaks at 47 and 56°2θ).

Lusvardi *et al*., on the other hand, did not find formation of fluorite (CaF_2) during SBF treatment, but their glasses formed calcite ($CaCO_3$) in SBF before forming apatite. The authors explain this by absence of a silica-gel layer in their glasses during SBF treatment, which is often considered to activate apatite nucleation, so that while formation of apatite is thermodynamically favoured, apatite formation is retarded resulting in formation of calcite due to kinetic effects [27]. However, the authors used Dulbecco's modified Eagle's medium (DMEM) with a HCO_3^- concentration ten times higher than that of SBF according to Kokubo [14], and this could favour formation of calcite rather than apatite or fluorite.

Often changes in glass behaviour (reactivity, degradation, pH or apatite formation) upon CaF_2 addition are attributed to the effect of fluoride [25-27], while in fact they can be explained by changes in the glass network (network

connectivity) due to unsuitable glass design: if CaF_2 is substituted for network modifier oxides such as CaO or Na_2O, it causes cross-linking of the silicate-network and an increased NC as shown previously in structural investigations [11] and molecular dynamics simulations [13]. As glass reactivity, degradation and apatite formation in bioactive glasses are highly susceptible to glass structure and NC, such glass design will make it difficult to determine if the changes are due to fluoride addition or due to changes in NC. We therefore added CaF_2 by the ratio of network former to network modifier (and thus the network connectivity) constant.

Table 2: Synthetic glass composition in mol%, theoretical network connectivity (NC) and experimental bioactivity (in terms of formation of an apatite layer in simulated body fluid) of glasses by Lusvardi *et al*. [13,27]

Glass	SiO_2	P_2O_5	CaO	Na_2O	CaF_2	NC
H	46.2	2.6	26.9	24.3	-	2.12
HNaCaF2 5%	46.2	2.6	26.9	19.3	5.0	2.34
HNaCaF2 10%	46.2	2.6	26.9	14.3	10.0	2.55
HNaCaF2 15%	46.2	2.6	26.9	9.3	15.0	2.77
HCaCaF2 5%	46.2	2.6	21.9	24.3	5.0	2.34
HCaCaF2 10%	46.2	2.6	16.9	24.3	10.0	2.55
HCaCaF2 15%	46.2	2.6	11.9	24.3	15.0	2.77

The results by Lusvardi *et al*. [27] show that all glasses in their series (up to 15 mol% CaF_2) form apatite according to XRD within 15 days in SBF solution. However, due to their glass design (CaF_2 added in exchange for CaO and Na_2O, respectively) NC values for glasses containing 10 mol% CaF_2 or above are ≥ 2.55. If we take the value of a NC = 2.4 as the cut off for bioactivity [12], we do not expect these glasses to form apatite in body fluids. NC values of above 2.4 describe a glass with 40% Q^3 species, which is a highly polymerised network that does not degrade easily in aqueous solutions and thus are not expected to form apatite. On the other hand it was shown that the phosphate phase of the glass structure has a huge impact on bioactivity of the glasses [23], as phosphate is present in an orthophosphate phase and does not form part of the actual silicate-network [11]. And an increase in phosphate content was shown to drastically increase bioactivity while limiting the pH rise in aqueous solutions [23]. We therefore conclude that the glasses by Lusvardi *et al*. [27] show bioactivity despite high network connectivity due to an increased phosphate content. This suggests that increasing the phosphate content in our glass system could increase the ability of the glasses to form apatite in physiological solutions.

Conclusions

Our results show that addition of fluoride results in formation of fluorapatite in simulated body fluid which is more acid resistant than carbonated hydroxyapatite and therefore fluoride-containing bioactive glasses are particularly interesting for applications in dentistry. However, our results show that high fluoride-content glasses in our system mainly form fluorite (CaF_2) in SBF, and formation of apatite is reduced compared to the fluoride-free composition. This could be

overcome by increasing the amount of phosphate in the glasses, as the release of phosphate would affect the supersaturation in SBF and thereby favour apatite deposition.

References

[1] Kokubo T, Takadama H. How useful is SBF in predicting in vivo bone bioactivity? Biomaterials 2006;27:2907-2915.

[2] Webster TJ, Ergun C, Doremus RH, Siegel RW, Bizios R. Specific proteins mediate enhanced osteoblast adhesion on nanophase ceramics. Journal of Biomedical Materials Research 2000;51:475-483.

[3] Hench LL. The story of Bioglass®. Journal of Materials Science: Materials in Medicine 2006;17:967-978.

[4] Towler MR, Crowley CM, Murphy D, O'Callaghan AMC. A preliminary study of an aluminum-free glass polyalkenoate cement. Journal of Materials Science Letters 2002;21:1123-1126.

[5] Tai BJ, Bian Z, Jiang H, Greenspan DC, Zhong J, Clark AE, Du MQ. Anti-gingivitis effect of a dentifrice containing bioactive glass (NovaMin®) particulate. Journal of Clinical Periodontology 2006;33:86-91.

[6] Thuy TT, Nakagaki H, Kato K, Phan AH, Inukai J, Tsuboi S, Nakagaki H, et al. Effect of strontium in combination with fluoride on enamel remineralization in vitro. Arch Oral Biol 2008;53:1017-1022.

[7] Featherstone JDB. The science and practice of caries prevention. Journal of the American Dental Association 2000;131:887-899.

[8] Position of the American Dietetic Association: The impact of fluoride on health. Journal of the American Dietetic Association 2005;105:1620-1628.

[9] Vestergaard P, Jorgensen NR, Schwarz P, Mosekilde L. Effects of treatment with fluoride on bone mineral density and fracture risk - a meta-analysis. Osteoporosis International 2008;19:257-268.

[10] Aaseth J, Shimshi M, Gabrilove JL, Birketvedt GS. Fluoride: A toxic or therapeutic agent in the treatment of osteoporosis? Journal of Trace Elements in Experimental Medicine 2004;17:83-92.

[11] Brauer DS, Karpukhina N, Law RV, Hill RG. Structure of fluoride-containing bioactive glasses. Journal of Materials Chemistry 2009;19:5629-5636.

[12] Hill R. An alternative view of the degradation of bioglass. Journal of Materials Science Letters 1996;15:1122-1125.

[13] Lusvardi G, Malavasi G, Cortada M, Menabue L, Menziani MC, Pedone A, Segre U. Elucidation of the structural role of fluorine in potentially bioactive glasses by experimental and computational investigation. Journal of Physical Chemistry B 2008;112:12730-12739.

[14] Kokubo T, Kushitani H, Sakka S, Kitsugi T, Yamamuro T. Solutions able to reproduce *in vivo* surface-structure changes in bioactive glass-ceramic A-W. Journal of Biomedical Materials Research 1990;24:721-734.

[15] Toby BH. EXPGUI, a graphical user interface for GSAS. Journal of Applied Crystallography 2001;34:210-213.

[16] Massiot D, Fayon F, Capron M, King I, Le Calve S, Alonso B, Durand JO, et al. Modelling one- and two-dimensional solid-state NMR spectra. Magnetic Resonance in Chemistry 2002;40:70-76.

[17] Bohner M, Lemaitre J. Can bioactivity be tested in vitro with SBF solution? Biomaterials 2009;30:2175-2179.

[18] Lu X, Leng Y. Theoretical analysis of calcium phosphate precipitation in simulated body fluid. Biomaterials 2005;26:1097-1108.

[19] Kim CY, Clark AE, Hench LL. Early stages of calcium-phosphate layer formation in bioglasses. Journal of Non-Crystalline Solids 1989;113:195-202.

[20] Jones JR, Sepulveda P, Hench LL. Dose-dependent behavior of bioactive glass dissolution. Journal of Biomedical Materials Research 2001;58:720-726.

[21] LeGeros RZ, Trautz OR, Klein E, Legeros JP. 2 Types of carbonate substitution in apatite structure. Experientia 1969;25:5-7.

[22] Rey C, Combes C, Drouet C, Lebugle A, Sfihi H, Barroug A. Nanocrystalline apatites in biological systems: characterisation, structure and properties. Materialwissenschaft und Werkstofftechnik 2007;38:996-1002.

[23] O'Donnell MD, Watts SJ, Hill RG, Law RV. The effect of phosphate content on the bioactivity of soda-lime-phosphosilicate glasses. Journal of Materials Science-Materials in Medicine 2009;20:1611-1618.

[24] Jäger C, Welzel T, Meyer-Zaika W, Epple M. A solid-state NMR investigation of the structure of nanocrystalline hydroxyapatite. Magnetic Resonance in Chemistry 2006;44:573-580.

[25] Fujii E, Kawabata K, Yoshimatsu H, Hayakawa S, Tsuru K, Osaka A. Structure and biomineralization of calcium silicate glasses containing fluoride ions. Journal of the Ceramic Society of Japan 2003;111:762-766.

[26] Hench LL, Spilman DB, Hench JW, inventors; University of Florida, assignee. Fluoride-modified bioactive glass (Bioglass) and its use as implant material. US patent 4775646; 1988.

[27] Lusvardi G, Malavasi G, Menabue L, Aina V, Morterra C. Fluoride-containing bioactive glasses: Surface reactivity in simulated body fluids solutions. Acta Biomaterialia 2009;5:3548-3562.